Ultrasound in Med. & Biol., Vol. 34, No. 1, pp. 123–136, 2008

0301-5629/08/$–see front matter

ELSEVIER

doi:10.1016/j.ultrasmedbio.2007.06.023

● *Original Contribution*

AN EXPOSIMETRY SYSTEM USING TISSUE-MIMICKING LIQUID

TIMOTHY A. STILES, ERNEST L. MADSEN, and GARY R. FRANK
Department of Medical Physics, University of Wisconsin-Madison, Madison, WI, USA

(*Received* 21 *December* 2006; *revised* 9 *April* 2007; *in final form* 26 *June* 2007)

Abstract—Acoustic output measurements of diagnostic ultrasound scanners are currently performed in water and derated to approximate *in situ* values. The derating scheme ignores nonlinear propagation of sound waves and has been shown in previous numerical and experimental studies to tend to *underestimate* relevant pressure and intensity values in tissue mimicking media. This work describes an alternative method, which uses a tissue-mimicking liquid with attenuation coefficient slope of 0.3 dB/cm/MHz, speed of sound of 1540 m/s and nonlinearity parameter B/A of 7.5. The acoustic properties of this liquid are stable for at least 2 y after production. Initial results using a single M-mode configuration are presented. These results confirm that derating can significantly underestimate the pulse intensity integral and peak rarefactional pressure. (E-mail: tastiles@wisc.edu) **© 2007 World Federation for Ultrasound in Medicine & Biology.**

Key Words: **Acoustic output, Nonlinear propagation, Tissue mimicking, Exposimetry.**

INTRODUCTION AND LITERATURE

Before ultrasound scanners can be marketed in the United States, the U.S. Food and Drug Administration requires that measurements be performed to quantify the acoustic output of the system. Acoustic output parameters are currently measured in accordance with the Acoustic Output Measurement Standard for Diagnostic Ultrasound Equipment (known as the AOMS) (AIUM 2004). The AOMS defines parameters that are to be measured, and many of these definitions are summarized in Table 1 For a detailed description of these parameters, see the AOMS. The AOMS requires that measurements be conducted in water with the resulting values derated in an attempt to account for the significant difference in ultrasound attenuation between water and soft tissues. The derating factor corresponds to an attenuation coefficient slope of 0.30 dB cm^{-1} MHz^{-1}. Derating is accomplished by multiplying measured values of acoustic pressure by $\exp(-0.0345 \times f_c \times d)$, where f_c is the center frequency of the pulse in megahertz and d is the distance between the ultrasound source and hydrophone in centimeters. (The AOMS assumes intensity is proportional to the square of the pressure amplitude; thus intensity values are multiplied by $\exp(-0.0691 \times f_c \times d)$).

One should note that this derating scheme was developed for the purpose of comparing the ultrasound output of devices with different frequencies and focal characteristics to determine if a new device seeking marketing clearance from the United States Food and Drug Administration (FDA) is "substantially equivalent" to ultrasound devices on the market prior to 1976. The derating scheme was not intended to exactly predict intensities and pressures within biological tissues. The derating coefficient of 0.30 dB cm^{-1} MHz^{-1} corresponds to a "fetal-weighted average" of a number of tissue types. Thus, the derated values should not be expected to represent actual tissue levels.

The derating process ignores nonlinear propagation of ultrasound, which can be significant at the frequencies and intensities commonly employed by diagnostic scanners. (For a review of nonlinear propagation as it applies to diagnostic ultrasound see Duck (2002).) Several numerical studies have used computer modelling of ultrasound beams to show that the straightforward approach used in the AOMS may considerably *underestimate* acoustic output parameters in tissue due to nonlinear propagation effects. Cahill and Humphrey (2000) simulated the nonlinear propagation of a continuous-wave pressure field from a diagnostic transducer in water and tissue and compared the results in tissue with the derated results in water. The source was 1.0 cm by 1.5 cm (elevational by lateral) and had a center frequency of either 3 or 6 MHz. The lateral focus was chosen to be at

Address correspondence to: Timothy A. Stiles, Department of Medical Physics, University of Wisconsin-Madison, 1300 University Ave, Room 1530 MSC, Madison, WI 53706, USA. E-mail: tastiles@wisc.edu

Table 1. Summary of some acoustic output parameters.

Parameter	Definition
f_c	Center frequency; the mean of the two most widely separated frequencies with amplitude 3 dB below the peak
I_{SATA}	Spatial-average temporal-average intensity; the average intensity over the entire area of the pulse
I_{SPPA}	Spatial-peak pulse-average intensity: average intensity during a single pulse
I_{SPTA}	Spatial-peak temporal-average intensity: average intensity over all time
MI	Mechanical Index; indicator of the likelihood of causing cavitation or other mechanical biological effect MI $= p_r.3/\sqrt{f_c}$
P_1, P_2	The two distances from the source at which the PII is equal to one half the maximum PII
PD	Pulse Duration; 1.25 multiplied by the time for the integral of instantaneous intensity to increase from 10% to 90% of the value of the PII
PII	Pulse Intensity Integral; the time integral of the instantaneous intensity in a single pulse: $\mathrm{PII} = \frac{\int_{t_1}^{t_2} v_h^2(t)\,\mathrm{d}t}{10^4 \rho_0 c_0 M_L^2(f_c)}$
PRF	Pulse repetition frequency; inverse of the period between identical pulses
p_r	Peak rarefactional pressure; most negative pressure in a waveform $p_r = \mathrm{abs}(\min(\frac{v_h(t)}{M_L(f_c)}))$
p_c	Peak compressional pressure; most positive pressure in a waveform $p_r = \max(\frac{v_h(t)}{M_L(f_c)})$
z_{max},PII	axial distance to maximum PII

$v_h(t)$ is the voltage produced by the hydrophone as a function of time for a particular measurement location; $M_L(f)$ is the frequency dependent hydrophone calibration constant (in units of V/Pa). The definitions given for p_c and p_r are correct only if the hydrophone/preamp combination does not invert the signal.

Detailed explanation of each is available in the AOMS (AIUM 2004)

8.0 cm with an elevational focus at 5.0 cm. For this study, tissue was chosen to have the same propagation speed as water but to have an attenuation of 0.30 dB cm^{-1} MHz^{-1}. The results of this study indicate that derated measurements of the spatial peak temporal average intensity (I_{SPTA}) may be as little as 50% of the value when nonlinear propagation is correctly accounted for. The Mechanical Index (MI) showed a smaller discrepancy, the MI in derated water being as little as 80% of the correct value. It is noted in this study that the simulated wave propagating in tissue does not develop shock wave characteristics while that propagating in water does. Thus, it may be that the simulated ultrasound wave propagating in tissue undergoes less nonlinear attenuation than the wave propagating in water. A similar study modelled the acoustic pressure field from the ATL HDI 3000 scanner using a P3-2 transducer operating at 2 MHz (Christopher 1999). This study also found a substantial difference between simulated values of the MI in tissue and simulated derated values in water with the derated water values being about 90% of the values in tissue. A third study (Divall and Humphrey 2000) used the Bergen code (Berntsen 1990) with some additional modelling of transducer self-heating and metabolic heat generation to calculate heat generation in an obstetrical model using diagnostic ultrasound pulses. This study found that when taking nonlinear propagation into account, heating at the location of the fetus could be twice as much as when linear propagation was assumed (increase of 1.25°C versus 0.58°C, respectively).

There are at least two experimental studies that have investigated measuring the acoustic output through a tissue-mimicking material with comparison to derated measurements in water. One of these (Szabo et al. 1999) used water-saturated extra firm organic tofu as a measurement medium, which has a propagation speed of 1520 m/s and an attenuation coefficient of 0.75 $f^{1.25}$ dB cm^{-1}, where f is the frequency in MHz. The ultrasound source was a circularly symmetric 5 MHz, 10 mm diameter, single element transducer with a 10 cm radius of curvature. Because of the discrete nature of the thicknesses of the sample, measurements were obtained using a hydrophone at 3, 4, 5 and 6 cm from the source. The results indicate that derated measurements obtained in water for the peak rarefactional pressure (p_r) and temporal average intensity (I_{TA}) were as little as 33% of those values with the tofu in place. Note that the tissue-mimicking material in this case had an attenuation coefficient slope more than twice the 0.3 dB cm^{-1} MHz^{-1} value recommended for derating and this may have influenced the degree to which the derated values in water disagree with the values through tofu.

The other experimental study of nonlinear propagation effects of acoustic output measurements was performed by MacDonald and Madsen (1999). The acoustic source for this study was an Acuson Sequoia clinical diagnostic scanner with an 1.5 linear array (Acuson Corporation of Mountain View, CA, USA is now Siemens Medical Solutions, Malvern, PA, USA.) This study measured the acoustic output from this system in water and in a tissue-mimicking liquid composed of diluted condensed milk with thimerosal as a preservative. The propagation speed of the liquid was 1526 m/s, the average attenuation coefficient slope was 0.27 dB cm^{-1} MHz^{-1} and the B/A of the material was 5.7. Two sets of data are presented in this study, both at 5 MHz, but at different focal depths, *viz.,* 2.0 cm and 7.0 cm. The results showed a significant difference in maximum pulse intensity integral (PII) and rarefactional pressure with a 7 cm focus, the values in tissue-mimicking (TM) liquid being about twice the derated values in water for both parameters. With a 2 cm focal depth, the derated values in water were approximately equal to or slightly

greater than the corresponding values in the tissue-mimicking medium. A significant problem that was encountered in this study was that over time (days), immersing the hydrophone in the tissue-mimicking liquid degraded the gold electrodes of the hydrophone and decreased the hydrophone response over time. Hydrophones are delicate instruments that are easily damaged and need to only be used in deionized distilled water. Additionally, the acoustic properties of the TM liquid used in this study were shown to change over time (days) as the lipid content of the evaporated milk rose to the surface. This change over time discourages replacing water with this TM liquid in exposimetry systems.

A previous article (Stiles et al. 2005) detailed the production of a tissue-mimicking liquid based on fat-free milk (also known as "skim milk") that eliminates the change in acoustic properties over time; the attenuation and speed of sound of this liquid were stable for more than two years. In the present report, we present an apparatus and measurement methodology that can be used to directly measure acoustic output parameters in this tissue-mimicking liquid without exposing the hydrophone to damage due to immersion in the liquid. Additionally, this apparatus allows for direct comparison of acoustic output parameter values in TM liquid and in water with derating applied. Results for a single M-mode configuration of a diagnostic scanner are presented. Measurements have been conducted on 47 additional configurations and the complete set of results is the subject of a future article.

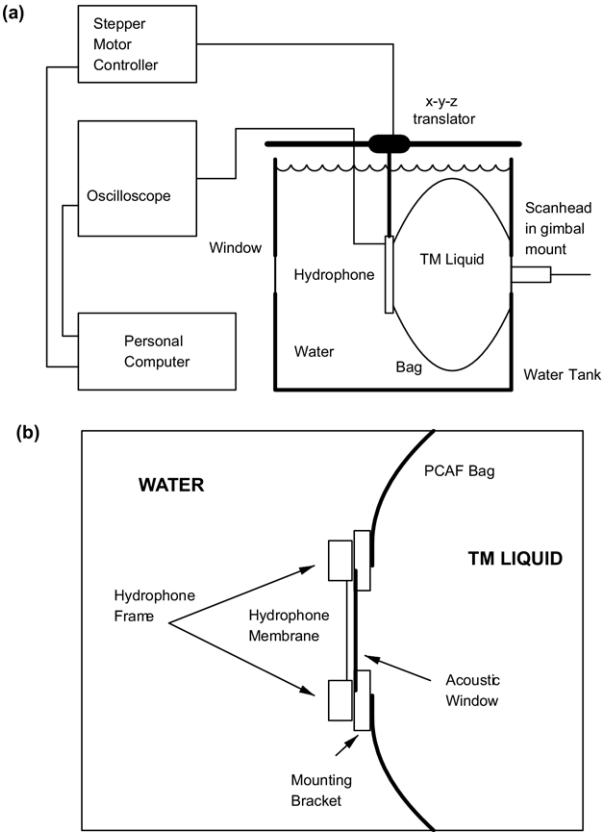

Fig. 1. (a) Schematic of entire apparatus used to measure acoustic output parameters in TM liquid or in water. (b) Detailed diagram of the exit window of the flexible sack, showing the acrylic frame and attachment of hydrophone mounting plate. Approximately 2 mm of water path exists between the exit window and the membrane hydrophone.

MATERIALS AND METHODS

This study focused on measuring the acoustic parameters for a non-auto-scan configurations, *i.e.,* M-mode and pulsed Doppler configurations, in which the ultrasound scanner only produces one beam line. This choice was made to avoid concern with beam overlap occurring in auto-scan modes. The number of adjacent acoustic beams present in auto-scan configurations dramatically increases the difficulty and time necessary to determine acoustic output parameters. However, the underlying physics of the situation remains unchanged whether there is one beam or several hundred and the results presented in this article should apply equally to B-mode and other modes.

Description of apparatus

A schematic of the measurement apparatus is shown in Fig. 1a. The major components of the complete system include: a water tank, an x-y-z translation system, a shielded, bilaminar membrane hydrophone, a digital storage oscilloscope, a diagnostic scanner and transducer probe and personal computer to control the position of the hydrophone and to record and analyze waveforms from the oscilloscope.

The tank is constructed from 1-cm thick plates of acrylic and has a total capacity of about 125 liters. The translation system consists of three mutually orthogonal linear positioning stages. Each stage consists of a screw driven linear positioner (UniSlide A40, Velmex, Inc., Bloomfield, NY, USA) and a stepper motor (Warner Electric, South Beloit, IL, USA). In the z-dimension, the rangè of the hydrophone is 60 cm; in the x- and y-dimensions (lateral and elevational dimensions of the scanhead, respectively), the range of motion is 15 cm. The translation system has a positioning accuracy of approximately 1 μm in all three dimensions. The bilaminar shielded hydrophone (originally produced Sonic Industries, Hatboro, PA, USA however, this manufacturer is no longer in operation, these hydrophones are currently manufactured by Sonora Medical Systems of Longmont, CO USA) has a 0.4 mm $\times$ 0.4 mm square active element. The hydrohpone is attached to the trans-

lator using an in-house produced gimbal mount with ±15° range in the two rotation axes. The two rotation axes intersect and one is vertical and the other is horizontal.

The oscilloscope trigger signal was generated using a "pick-up coil" placed near the surface of the scanhead such that the electric signal applied to the piezoelectric elements produced an induced voltage in the coil. The coil consists of ten turns of insulated solid 24 gauge (AWG) wire. The turns are nearly circular with a diameter of about 3 cm. The coil is placed in direct contact with the scanhead housing along the side of the housing near the face of the scanhead with the plane of the coil parallel to the scanhead housing. The signal from the hydrophone was digitized at 500 megasamples per second by a digital oscilloscope (Model LT342, LeCroy Corporation, Chestnut Ridge, NY USA). About 100 waveforms were averaged by the oscilloscope to reduce contributions from electronic noise. The averaged waveforms were transferred to a personal computer (custom-built) *via* the General Purpose Interface Bus (GPIB). The PC also controlled the translation of the hydrophone in three simultaneous dimensions using a Velmex VP9000 stepper motor controller (Velmex, Inc., Bloomfield, NY USA) connected to the computer *via* serial interface. In-house C++ programs were used to control the oscilloscope and stepper motor controller and to acquire data. Off-line analysis of the recorded waveforms was performed using the *Mathematica* computer algebra system (Wolfram Research, Inc., Champaign, IL USA).

Throughout this study, the TM liquid used for measurements was skim milk concentrated by a factor of about 3 *via* ultrafiltration and preserved by autoclaving at 120°C for 15 min and adding 5% vol/vol formalin (Fisher Chemical, Fairlawn, NJ USA), as described in Stiles et al. (2005). The acoustic properties of this liquid were measured at 22°C using narrow-band through-transmission techniques. The speed of sound at 5.0 MHz was 1538 ± 1 m/s and nonlinearity parameter, B/A, was 7.5 ± 0.5. The attenuation coefficient was measured at nine frequencies between 1.0 and 20.0 MHz; the results are displayed in Fig 2. A least-square fit of the attenuation coefficient to the power-law model $\alpha_0 f^n$, where f is the frequency resulted in $\alpha_0 = 0.25 \pm 0.01$ dB cm^{-1} MHz^{-n} where $n = 1.15 \pm 0.02$ This fit is given by the solid line in Fig 2.

It is recommended by the manufacturer that the hydrophone not be placed into any medium other than deionized distilled water. MacDonald and Madsen (1999) observed a decrease in hydrophone sensitivity after immersing a membrane hydrophone for significant periods of time (days) in a TM liquid similar to that used in this study. This degradation was likely caused by the prolonged immersion of the hydrophone in the TM liquid. It may be possible to prevent this degradation by only allowing the hydrophone to be immersed for shot periods of time in the TM liquid and then rinsed with distilled, deionized water. Additionally, the stability of the TM liquid used in the present report (Stiles et al. 2005) was only tested with the liquid contained in a closed air-free sample cylinder. It is likely that direct exposure to air would hasten any degradation of the liquid over time. There are two routes through which such degradation could occur. The preservative in the liquid could eventually be overcome through constant exposure to new microbes. Perhaps even more important, the water and formalin component of the TM liquid can evaporate over time. Therefore, some method of maintaining the TM liquid in an air-free sealed container with the hydrophone external to this container is considered essential to maintaining long-term stability of the TM liquid and the hydrophone.

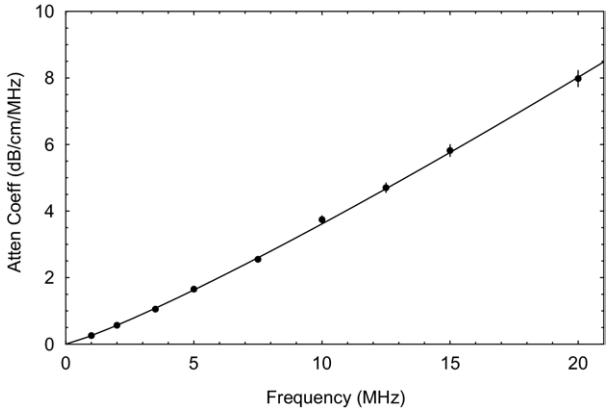

Fig. 2. Attenuation coefficient of TM liquid at nine frequencies spanning 1.0 to 20.0 MHz. The solid curve is fit to the "power-law" model $\alpha_0 f^n$ with fit parameters $\alpha_0 = 0.25 \pm 0.01$ dB cm^{-1} MHz^{-n} where $n = 1.15 \pm 0.02$

The method used to contain the TM liquid for this study is to enclose the TM liquid in a flexible sack of plastic-coated aluminum foil (PCAF) that is suspended in the water tank. PCAF was chosen because of its low vapor permeability and low reactivity with organic compounds. This material (hereafter referred to as "APC White", American Packaging Company, Lawrenceville, GA, USA) consists of a sandwich of layers: 12 μm polyester containing white dye, 17 μm polyethylene, 9 μm aluminum and 60 μm ScotchPak® plastic film. Approximately 10 liters of tissue-mimicking liquid was confined within this sack. This method of confining the TM liquid allows for almost all of the acoustic path to be in the TM liquid, with only a small path length (approximately 2 millimeters) in water between the exit window of the sack and the hydrophone. The minimum distance between the ultrasound source and hydrophone is about

1.4 cm. The maximum path length is approximately 30 cm.

Two acoustic "windows" of a different type of PCAF have been placed in the tank walls on opposite sides of the tank to allow ultrasound to pass into the tank. All three windows (entrance and exit to TM liquid sack and entrance to tank into water) are constructed of Pechiney Spec 151 (Pechiney, Inc., Chicago, IL USA). This material is designed for use in the food industry and consists of a 50 micron thick layer of ethylene vinyl acetate (EVA), a 12 micron layer metalized polyethylene and a 50 micron layer of EVA. This material was chosen based on its superior acoustic transmission properties (described below) while still being an effective vapor barrier. Figure 1b provides a depiction of the complete exit window with the hydrophone in place.

Transmission coefficient of acoustic windows

As an acoustic wave passes from one medium into another, the energy present in the initial wave is partially transmitted into the second medium and partially reflected back into the first medium. The amplitudes of the pressures of the transmitted and reflected waves depend on the physical properties of the media and of any acoustic "window" between the media. The method proposed in this work requires the ultrasound beam to traverse two media interfaces to obtain results in TM liquid. At each of these interfaces the amplitude of the wave will change, and such changes should be accounted for in the final values of the acoustic output parameters. The transmission coefficient of the window material is a frequency dependent, complex (amplitude and phase) parameter.

The transmission coefficient of the window material had been previously measured in our lab to assess the suitability of this material as a window material for ultrasound phantoms. These measurements (described in detail below) were conducted with water on both sides of the window using several pairs of single element transducers. The apparatus described above, however, involves the transducer being in direct contact (via coupling gel) with the window material at the entrance windows.

It has been assumed by us that the transmission coefficient with the clinical transducer in direct contact *via* ultrasound coupling gel (Aquasonic 100, Parker Laboratories, Fairfield, NJ, USA) with the window material is not substantially different from the case when there is a layer of water between the transducer and the window material. To test this assumption, a clinical linear array operating in M-Mode (Siemens Sonoline Antares with VFX9-4 scanhead, Siemens Medical Solutions, Malvern, PA, USA) was positioned at the surface of a tank of water with the beam directed downward to the membrane hydrophone positioned on the beam axis near the focal region. A horizontal

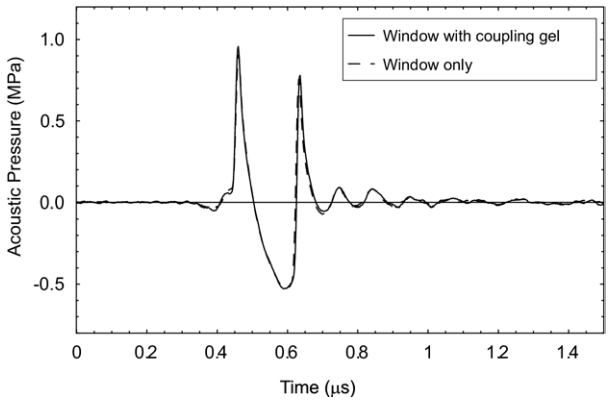

Fig. 3. Pressure waveforms with clinical transducer in direct contact with acoustic window material *via* coupling gel (solid curve) and with window material approximately 1 cm from transducer face with water between transducer and window material (dashed curve).

sample of the window material could be placed at any position between the scanhead and hydrophone, including in direct contact with scanhead *via* coupling gel. Comparison of waveforms at nominal frequencies of 4 and 9 MHz with the window material about 1 cm from the transducer face or in direct contact with the scanhead showed differences in p_r of less than 0.7% and differences in PII of less than 3%. We conclude that the coupling gel does not substantially alter the acoustic transmission properties of the window material relative to the case in which the transducer is in water. Figure 3 shows the two waveforms recorded for the nominal 9 MHz case. Based on these results, it is reasonable to use the water-through-Pechiney-film-to-water or water-though-Pechiney-film-to-TM-liquid transmission coefficients to account for the direct contact transmissions into either the water or TM liquid sides of the tank, respectively.

The correction to the transmitted pulse to eliminate the effect of transmission through the acoustic window can be achieved through the use of a digital filter that is the inverse of the frequency dependent transmission coefficient at each frequency involved. The waveform that is transmitted through the entrance window only contains the fundamental frequency range while the waveform transmitted through the exit window of the TM liquid-filled sack contains many harmonics that were generated in the propagation medium between the transmission into the tank and reception of the signal. Therefore, unlike the case of the exit window, the correction for the entrance window should include only those frequencies that were present at the entrance window. This can be done by determining a "cutoff frequency," f_{cutoff}, such that the frequency content present at the entrance window is less than f_{cutoff}. To determine the value of f_{cutoff}, the hydrophone was positioned as close as possible to the entrance

window in the water side of the tank (approximately 1 mm). The spectrum at this location was analyzed to determine f_{cutoff}, usually taken to be the −20 dB point on the high frequency side of the spectrum.

If $v_{TM}(t)$ is the measured voltage waveform from the hydrophone when the ultrasound beam passes through the TM liquid, the transmission-corrected (tc) waveform is given by:

$$v_{TM,tc}(t) = \begin{cases} \mathcal{F}^{-1}\left(\frac{1}{T_{ent}(f)} \cdot \frac{1}{T_{exit}(f)} \cdot \mathcal{F}\left(v_{TM}(t)\right)\right), & f \le f_{\text{cutoff}} \\ \mathcal{F}^{-1}\left(\frac{1}{T_{exit}(f)} \cdot \mathcal{F}\left(v_{TM}(t)\right)\right), & f > f_{\text{cutoff}} \end{cases} \quad (1)$$

where $T_{ent}(f)$ and $T_{exit}(f)$ are the complex, frequency dependent transmission coefficients of the entrance (water to TM liquid) and exit (TM liquid to water) windows, respectively and $\mathcal{F}$ and $\mathcal{F}^{-1}$ indicate the forward and inverse Fourier transform, respectively. A similar correction is performed for waveforms recorded in water. However, these signals only pass through an entrance window so we have

$$v_{w,tc}(t) = \mathcal{F}^{-1}\left(\frac{1}{T_{water}(f)} \cdot \mathcal{F}\left(v_w(t)\right)\right), \; f \le f_{\text{cutoff}} \quad (2)$$

where $v_w(t)$ is the measured voltage waveform in water and $T_{water}(f)$ is the measured water to water complex transmission coefficient of the membrane with water.

The following subsections present details of the measurement of the complex (amplitude and phase) transmission coefficient of the material used as acoustic windows in the apparatus. Measurements were performed with water on both sides of the window material as well as with water on one side and TM liquid on the other side. Also, only perpendicular incidence was considered.

Transmission coefficient measurements with water on both sides of window

The transmission coefficient of the window material (perpendicular incidence) was measured from 1 to 50 MHz using narrowband and broadband methods. To cover this frequency range, eight pairs of transducers were utilized, the nominal center frequencies of the transducer pairs used were 1.0, 2.25, 3.5, 5.0, 7.5, 10.0, 15.0 and 30.0 MHz. To reduce errors associated with diffraction and phase-cancelation effects, each receiving transducer has a smaller aperture than the corresponding transmitting transducer.

In the narrowband method, the transmitting transducer was excited by a quasi-continuous wave pulse consisting of 30 cycles at a specific frequency. To fully cover the frequency range, measurements were conducted at 98 frequencies separated by 0.5 MHz (*i.e.,* 1.0 MHz, 1.5 MHz, 2.0 MHz, . . . , 50.0 MHz). The received waveforms with and without the window material present between the transducers were analyzed to determine the peak-to-peak amplitude and total time between the generation and reception of the ultrasound pulse. The magnitude of the transmission coefficient is obtained by dividing the peak-to-peak amplitude with the window material present by the peak-to-peak amplitude without the window present. The phase of the transmission coefficient is equal to the angular frequency ($2\pi f$) multiplied by the time shift occurring when the window material is introduced between the transducers. In general, this time shift is very small, with a value of several tens of nanoseconds.

In the broadband method, the transmitting transducer was excited by a narrow voltage spike provided by a Panametrics model 5052PR (Waltham, MA USA) pulser receiver. The received signal was digitized at 500 MHz using a LeCroy LT342 digital storage oscilloscope (Chestnut Ridge, NY USA). Data was collected from each of the eight pairs of transducer and analyzed only over the −12 dB bandwidth of the signal. The amplitude of the transmission coefficient is obtained by dividing the amplitude at each frequency of the Fourier transform of the received signal with the sample in the path by the amplitude at each corresponding frequency of the Fourier transform of the signal without the sample. The phase of the transmission coefficient can be obtained by subtracting the phase of the Fourier transform of the reference signal from the phase of the Fourier transform of the signal with the sample present. Because of the inherent 2π ambiguity in phase, care must be taken when performing this computation to eliminate jumps of 2π (Marple, 1987).

The results of broad band and narrow band measurements of the amplitude and phase of the transmission coefficient for the window material are shown in Fig. 4. The solid black squares are the 338 data points obtained using the broad band method, the grey squares are the 153 data points obtained using the narrow band method. (Note that there was some overlap in frequency range between each transducer pair, therefore there are more narrow band data points than the 98 discrete frequency values.) The solid curves in this figure is a least squares fit to the model of transmission through a multiple layer material at perpendicular incidence given by Brekhovskikh (1980) (page 26, eq 3.47), including the effect of attenuation in each of the media. The values of speed of sound and density of the layers of ethylene vinyl acetate (EVA) found by this fit agree well with published values (Selfridge 1985). This model performs reasonably well in reproducing the measured results. The largest

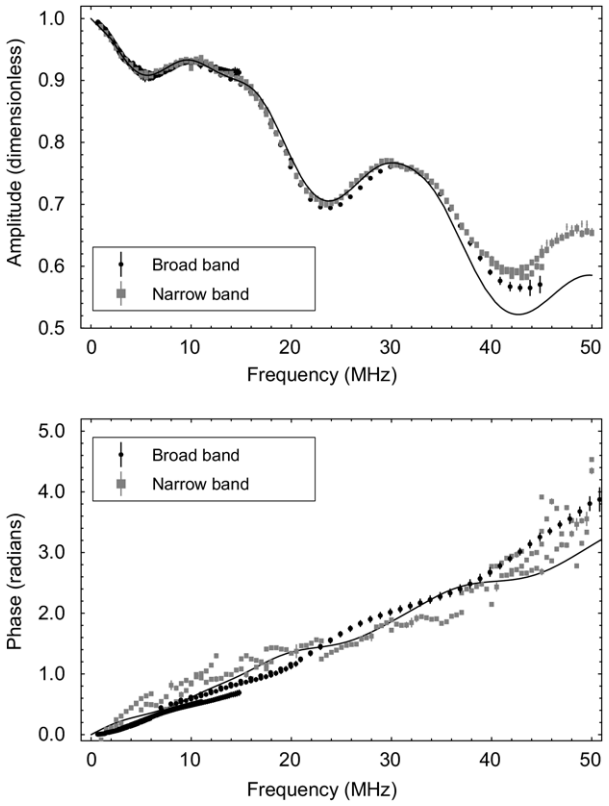

Fig. 4. Amplitude (a) and phase (b) of transmission coefficient in water for the acoustic window material (Pechiney Spec 151). Solid curve is fit to the model (Brekhovskikh 1980, eq 3.47).

discrepancy between the model and the data is in the region above 35 MHz. The differences between the model fit and the data may be due to effects that are not included in the model, such as the attenuation of the components of the plastic coated aluminum foil not following a power law model at these frequencies. Because the model deviates from the measured values at high frequencies, a 12 order polynomial fit was used to provide corrections for the transmission coefficient.

Water on one side and TM liquid on the other side of the window

Transmission coefficients with water on one side of the window and TM liquid on the other side must also be measured. With dissimilar liquids on either side of the window material, it is not possible to directly measure the effect of the window material since the liquids would mix at the interface in the absence of the window material. Instead, the relative transmission coefficient between the multilayered plastic coated aluminum foil and and a homogenous layer of another material was measured and then a correction factor applied to convert this relative transmission coefficient to absolute transmission coefficient. Polyethylene (U.S. Plastic Corporation, Lima, OH USA) was chosen as the reference material because it has an acoustic impedance that is relatively close to that of water and that of the TM liquid. The acoustic impedance of polyethylene is 1.76×10^6 rayl, compared to 1.49×10^6 rayl for water and 1.62×10^6 rayl for TM liquid. Therefore, the amplitude of the transmission coefficient with a very thin polyethylene window present is very close to that in the absence of the polyethylene window. Similarly, the phase of the transmission coefficient through such a window is proportional to angular frequency with a slope equal to the thickness of the window divided by the speed of sound in the window (*i.e.,* a slope equal to the time shift upon passing through the window).

For these measurements the amplitude through the sample window material was compared with a well-characterized simple material, a thin sheet (15 μm) of polyethylene (the reference window). The procedure involves a "tank within a tank" approach, in which a cylindrical tank is inside of a rectangular tank. The inner tank was approximately 40 cm in diameter and 15 cm in height. The outer tank was 100 cm by 50 cm by 15 cm. The space between the inner and outer tank walls was filled with water, the inner tank was filled with TM liquid. The inner tank had two windows, the reference window of 15 μm-thick polyethylene and the sample window of Pechiney Spec 151 window material. The inner tank could be rotated allowing for either of these windows to be positioned between the transmitting and receiving transducers without the need for adjusting the positions of the transducers.

Using this arrangement one can measure the transmission coefficient with the Pechiney material in place relative to the transmission coefficient with the 15 μm polyethylene in place. The transmission coefficient of the 15 μm polyethylene was measured from 1 through 50 MHz with water on both sides; magnitude values were never less than 0.98. Thus the polyethylene has very little effect. Nevertheless, the reference transmission coefficients for 15 μm polyethylene with water on one side and TM liquid on the other were computed for a three-layer medium using available propagation speed, density and attenuation coefficient for the soft polyethylene. We can use the recorded amplitude and time of flight with the sample window or reference window in place to determine the magnitude and phase of the transmission coefficient of the sample window. The magnitude is given by

$$T_s(f) = \frac{A_s(f)}{A_r(f)} \cdot T_r(f) \tag{3}$$

and the phase by

$$\phi_s = \omega \cdot (t_s - t_r) + \phi_r \quad (4)$$

where f is the frequency, T_s (T_r) is the magnitude of the transmission coefficient of the sample (reference) window, ϕ_s (ϕ_r) is the phase of the sample (reference) window and $\omega = 2\pi f$ is the angular frequency. A_s and A_r are the measured voltage amplitudes of the received signal with the sample window in place or with the reference window in place, respectively, and t_s and t_r are the times of flight between the transmitter and receiver through the sample window or reference window, respectively. The quantities T_r and ϕ_r are the *calculated* magnitude and phase of the transmission coefficient for TM liquid though the reference window and into water (or water into reference window into TM liquid). These calculations were obtained using the equation for a single layer described in Brekhovskikh (1980)(page 15) using measured values for the density and speed of sound in polyethylene.

As with the measurements of the transmission coefficient with water on both sides of the window, both broad band and narrow band techniques were used to determine the magnitude and phase of the transmission coefficient with water on one side and TM liquid on the other. These results were then fit to a polynomial. The magnitude of the transmission coefficient from TM liquid through the window material and into water is similar to that from water to water except for about a 4% difference due to the difference in acoustic impedance between water and the TM liquid. The results of polynomial fits to data for each of the three cases (water to water, TM liquid to water, and water to TM liquid) are depicted in Fig. 5.

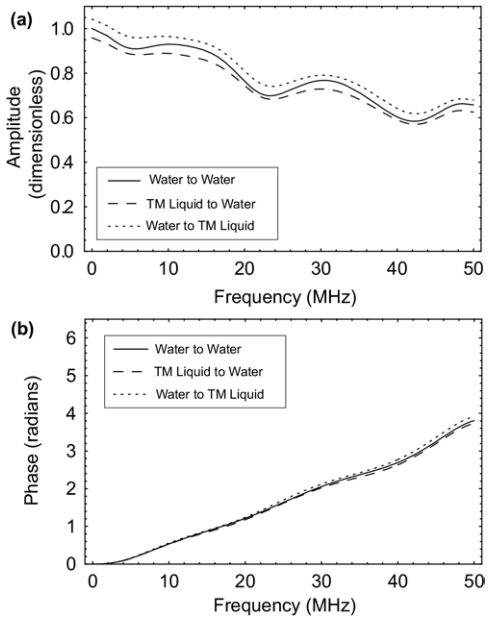

Fig. 5. Polynomial fits of amplitude (a) and phase (b) of the transmission coefficient for the acoustic window material (Pechiney Spec 151) for three cases of transmission: water on both sides of window (solid curve); transmission from TM liquid through the window and into water (dashed curve) and transmission from water through the window and into TM liquid (dotted curve).

Measurement procedure

The procedure for performing measurements of acoustic output parameters in water with derating applied did not vary significantly from that described in the acoustic output measurement standard. The measured waveforms were corrected for the presence of the acoustic windows as described above. Additionally, in order to compare the derated values with those obtained in TM liquid, the derating coefficient was modified to correspond to the attenuation coefficient of the TM liquid at the center frequency (f_c) of the pulse, rather than the standard 0.30 dB cm^{-1} MHz$^{-1} \cdot f_c$. Acoustic output values derated according to this modified derating coefficient are referenced with a subscript "der" rather than the usual ".3", such as $p_{r,der}$ for the derated peak rarefactional pressure at the location of maximum pulse intensity integral (PII). Acoustic output values measured in TM liquid are similarly referenced with a subscript "TM". Variables with neither "der" nor "TM" as a subscript are values obtained in water with no derating applied.

One can translate the hydrophone in the lateral or elevational direction to obtain profiles in these dimensions. Also, a "raster" scan can be made, in which the hydrophone is scanned throughout a plane perpendicular to the beam axis by translating in the lateral direction across the plane, then translating slightly in the elevational direction and translating back across the plane laterally. This is one of the methods though which the AOMS specifies for the measurement of total power produced by an ultrasound scanner in a particular configuration. A scan of the acoustic field within one plane also allows for the determination of the transverse extent of the acoustic field.

The data collected over the raster of points are analyzed to determine the total power and the spatial-average temporal-average intensity (I_{SATA}). Total power at some distance from the scanhead was determined by integrating the PII beam profile over the area of the beam to determine the total energy per pulse and then multiplying by the pulse repetition frequency. The spatial-average temporal-average intensity is defined as the total power divided by the beam area. The beam area can be measured by assuming that the beam is approximately elliptical in cross-section, measuring the -6 dB width of

the beam in the transverse and elevational dimensions and using the formula for the area of an ellipse.

Uncertainties in parameter values were estimated based on standard propagation of errors of the known uncertainties in hydrophone and oscilloscope calibrations. For derated values, the uncertainties in the values of α_0 and n were also computed and accounted for. However, the primary goal of this article is to present a comparison (*via* ratios) of values obtained in TM liquid to those obtained in water with derating applied, and since the hydrophone instrumental error is the same for water-derated and TM liquid cases, the uncertainties in the ratios of values in TM liquid to derated values in water do not include the (canceling) hydrophone error.

RESULTS

This section presents a complete description of the data collected from one M-mode configuration. The scanner used for this configuration was the Acuson Sequoia (now Siemens Medical, Seattle, WA USA) operating with the 6L3 scanhead. The displayed frequency of the scanner was 5.0 MHz and the displayed focal depth was 5.0 cm.

The positions of maximum PII in water with derating applied and in TM liquid were determined by translating the hydrophone along the beam axis. Figure 6a presents the waveforms corresponding to maximum PII in water with derating, and the waveform corresponding to maximum PII in TM liquid. These waveforms are very similar in most aspects except for amplitude, with no drastic changes in overall shape or pulse length. The sections of the waveforms with positive slope are much steeper than the sections with negative slope, indicating the formation of a shock wave. Additionally, in both media the compressional pressure is much greater than the rarefactional pressure. It is interesting to note that the acoustic-pressures of the waveforms near the beginning and end of the pulses are nearly identical; that is, the acoustic pressures of the first and last positive half-cycles in water with derating and TM liquid nearly coincide. Since these parts of the pulses have lower amplitude, it is probable that they undergo less nonlinear distortion than the central portions of the pulses.

The normalized spectra of these pulses are presented in Fig. 6b. In either water or TM liquid, considerable nonlinear propagation has occurred as evidenced by the presence of significant harmonic content. Because of frequency dependent attenuation, the main lobe of the spectrum of the pulse recorded in TM liquid is shifted slightly to the left (lower frequency) relative to the main lobe of the spectrum recorded in water. These shifts are even more dramatic for the higher harmonics; e.g., the peak frequency of the fifth harmonic is at 24.1 MHz in TM liquid and at 26.0 MHz in water. Also note that the relative amplitudes of the harmonics are smaller in TM liquid than in water by several decibels.

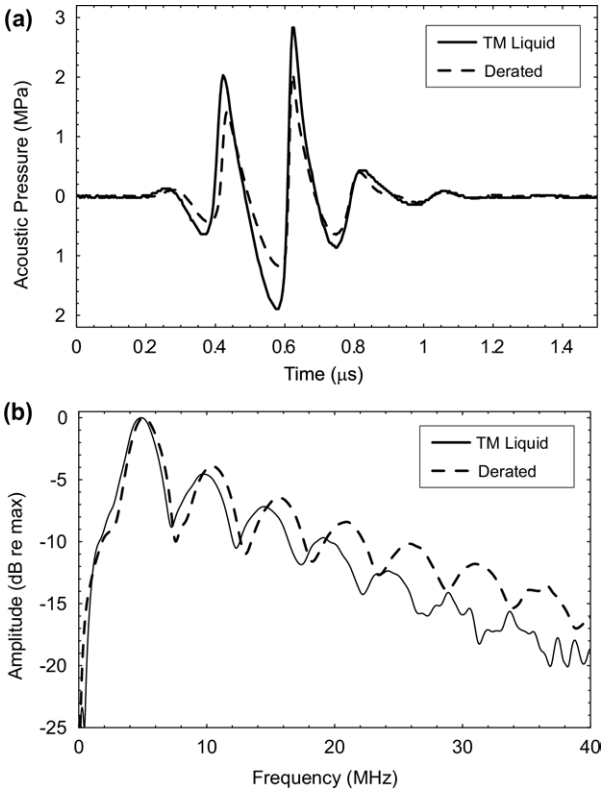

Fig. 6. Comparison of the pressure waveform (a) and spectral amplitude (b) in TM liquid (solid) to those in water with derating applied (dashed). Measurements were performed at the location of maximum PII in TM liquid and maximum derated PII in water. The scanner was an Acuson Sequoia with 6L3 scanhead operating in M-mode at 5.0 MHz with focal depth of 5.0 cm.

Table 2 provides the measured values of several acoustic output parameters. Recall that the ratios of pressures and intensities in the right column have uncertainties which do not include the instrumental uncertainty of the hydrophone because those uncertainties "divide out." This table includes values for the maximum PII ($PII_{\max}$), the distance from the source to the location of maximum PII ($z_{\max,PII}$), the center frequency, the pulse duration (PD), the pulse repetition frequency (PRF), the spatial peak temporal peak intensity (I_{SPTA}), the spatial peak pulse average intensity (I_{SPPA}), the peak rarefactional (p_r) and peak compressional pressure (p_c) at the location of maximum PII as measured in TM liquid and in water with derating of $0.25f^{1.14}$ applied. The "MI equivalent" is reported, which is defined in TM liquid as the measured p_r in MPa at the location of maximum PII divided by square root of the center frequency in MHz. In water, this value is defined as the derated p_r in MPa, with derating

Table 2. Values of acoustic output parameters, measured in TM liquid and in water with derating applied, for an Acuson Sequoia with a 6L3 scanhead operating in M-Mode at 5.0 MHz and 5.0 cm focal depth

Parameter	TM Liquid	Water, derated at $0.25f_c^{1.14}$ dB/cm	Ratio
PII_{max} ($\mu J/cm^2$)	34.7 ± 1.3	19.2 ± 0.8	1.81 ± 0.10
$z_{max,PII}$ (mm)	48.5 ± 0.2	50.0 ± 0.2	0.97 ± 0.01
f_c (MHz)	4.91 ± 0.05	5.15 ± 0.05	0.95 ± 0.02
PD (μs)	0.29 ± 0.01	0.34 ± 0.01	0.85 ± 0.02
PRF (Hz)	610 ± 10	610 ± 10	1.0 ± 0.0
I_{SPTA} (mW/cm^2)	21.2 ± 0.9	11.7 ± 0.5	1.81 ± 0.10
I_{SPPA} (W/cm^2	119 ± 5	57 ± 2	2.12 ± 0.13
p_r at $z_{max,PII}$ (MPa)	1.90 ± 0.04	1.17 ± 0.04	1.62 ± 0.07
p_c at $z_{max,PII}$ (MPa)	2.55 ± 0.04	2.06 ± 0.06	1.24 ± 0.04
MI equivalent	0.86 ± 0.02	0.52 ± 0.02	1.66 ± 0.07
Global maximum rarefactional pressure (MPa)	1.90 ± 0.04	1.28 ± 0.04	1.48 ± 0.05
Distance to global maximum rarefactional pressure (mm)	48.5 ± 0.5	19.5 ± 0.5	2.50 ± 0.07
Global maximum compressional pressure (MPa)	2.61 ± 0.03	2.27 ± 0.08	1.15 ± 0.05
Distance to global maximum compressional pressure (mm)	50.5 ± 0.5	50.5 ± 0.5	1.00 ± 0.05

The derating coefficient used for the water measurements corresponded to the measured attenuation coefficient of the TM liquid, *viz.* $0.25f_c^{1.14}$ dB/cm, where f_c is the measured center frequency in MHz. For this configuration, which produces a derating coefficient that is equivalent to an attenuation coefficient slope of 0.314 dB/cm/MHz, slightly greater than the canonical 0.30 dB/cm/MHz used in the AOMS.

The right-most column is the ratio of the value measured in TM liquid to the corresponding derated value measured in water. All uncertainties are estimated ignoring the effect of hydrophone calibration but including the effect of positioning and oscilloscope calibration.

coefficient of 0.25 $f^{1.14}$, divided by square root of the center frequency in MHz. Additionally, this table includes the values of the peak negative and peak positive pressures anywhere in the field and the spatial location at which those maximums occur.

In addition to recording the waveform at the location of maximum PII for each configuration, the waveforms along the beam axis were recorded and analyzed. This was accomplished by translating the hydrophone along the z-axis and recording waveforms at discrete locations. These waveforms were analyzed to provide axial profile plots of the various parameters. Figure 7 depicts the axial profile of the PII measured in water without derating applied, the PII measured in water with derating applied and the PII measured in TM liquid. The peak in these profiles corresponds to the particular lateral focusing applied in this configuration. The values measured in TM liquid are greater than those measured in water with derating applied for all values of distance from the source. Figures 8 and 9 depict the axial distribution of the rarefactional and compressional pressures, respectively. Figure 10 displays the ratios of each of these three parameters measured in TM liquid to that measured in water with derating applied.

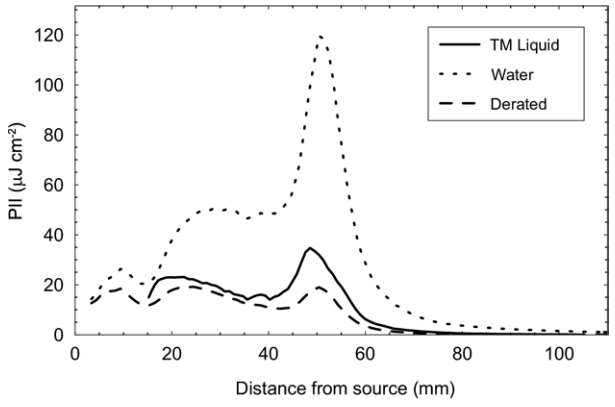

Fig. 7. Pulse intensity integral at various distances from the surface of the transducer measured in TM liquid (solid curve), water (dotted), and water with derating applied (dashed). The scanner was an Acuson Sequoia with 6L3 scanhead operating in M-mode at 5.0 MHz with focal depth of 5.0 cm.

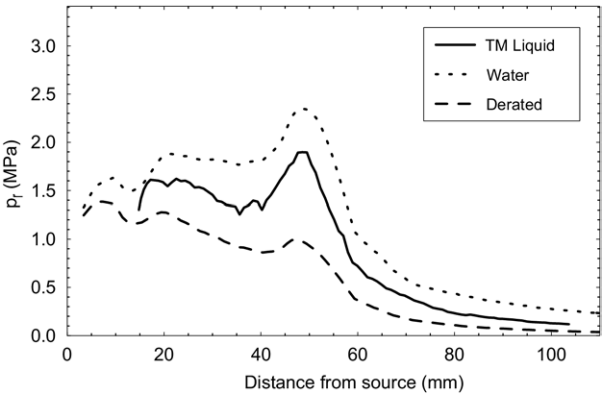

Fig. 8. Maximum rarefactional pressure (p_-) at various distances from the source, measured in TM liquid (solid curve), water (dotted) and water with derating applied (dashed). The scanner was an Acuson Sequoia with 6L3 scanhead operating in M-mode at 5.0 MHz with focal depth of 5.0 cm.

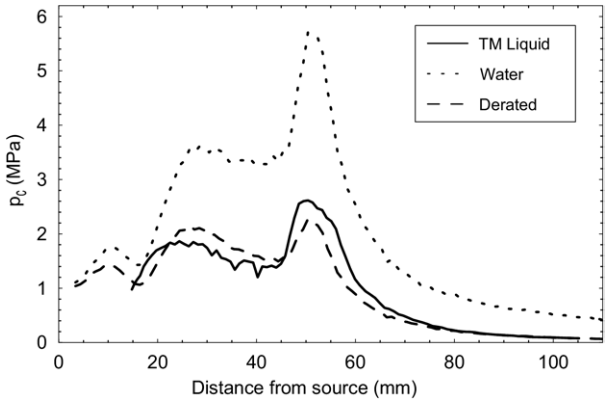

Fig. 9. Maximum compressional pressure (p_+) at various distances from the source, measured in TM liquid (solid curve), water (dotted) and water with derating applied (dashed). The scanner was an Acuson Sequoia with 6L3 scanhead operating in M-mode at 5.0 MHz with focal depth of 5.0 cm.

A raster scan was performed with a spacing between adjacent lateral or elevational points of 0.3 mm. The axial distance was the distance to the maximum PII in TM liquid, 50.0 mm. The entire scan covered a square area, 6 mm × 6 mm, centered at the maximum PII. Figure 11 presents a contour plot of the resulting PII distribution. The spacing between adjacent contours in this figure is 3 dB. The distributions are nearly identical for the case of water with derating applied and TM liquid. Table 3 provides values for some of the geometrical factors and total power for this configuration.

To assess the long-term repeatability of measurements conducted with this apparatus, the acoustic output parameters in TM liquid and water for this configuration were measured again 6 mo after the initial measurements. The results of the initial and repeated measurements in TM liquid are displayed in Table 4 These results indicate that the measurements on two different dates were within the estimated uncertainty from random errors in hydrophone position and oscilloscope recording.

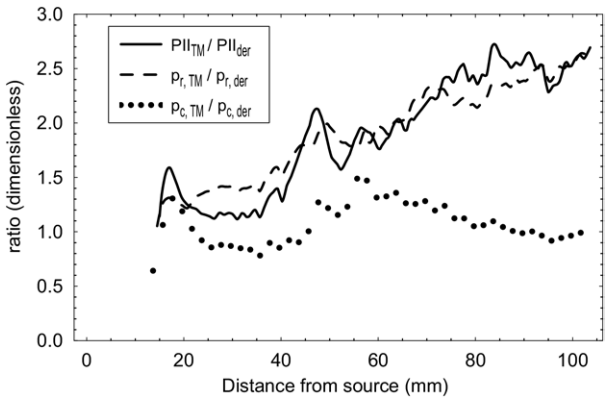

Fig. 10. Ratios of PII, p_+ and p_- in TM liquid to the corresponding derated value in water measured at various distances from the source. The scanner was an Acuson Sequoia with 6L3 scanhead operating in M-mode at 5.0 MHz with focal depth of 5.0 cm.

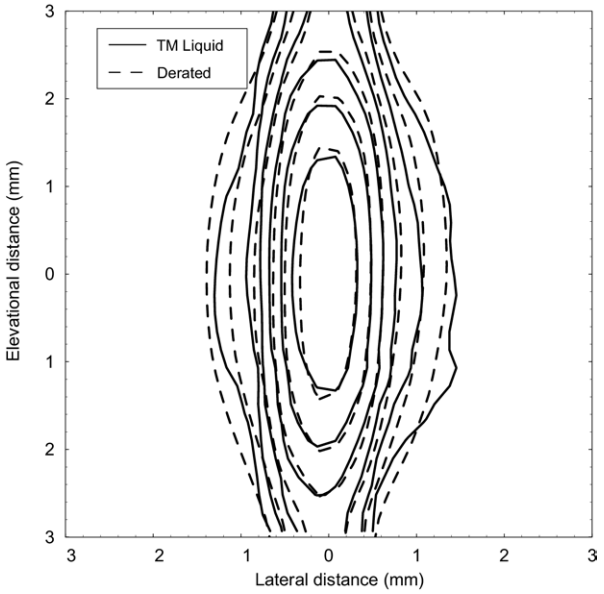

Fig. 11. Beam profile plots in TM liquid and in water. Each contour is separated by 3 dB from the adjacent contours. The axial distance corresponds to that of the maximum PII in TM Liquid.

Variation of drive voltage amplitude

Typically, diagnostic scanners allow direct control over the amplitude of the voltage signal used to excite the transducer elements. This control is variously known as the "drive voltage amplitude", "power output" or

Table 3. Values of acoustic output parameters related to beam geometry, measured in TM liquid and water with derating applied

Parameter	TM liquid	Water derated	Ratio
P1 (mm)	43.2 ± 0.5	45.3 ± 0.5	0.95 ± 0.02
P2 (mm)	55.7 ± 0.5	55.3 ± 0.5	1.01 ± 0.02
−6 dB width (lateral) (mm)	1.04 ± 0.05	0.98 ± 0.05	1.06 ± 0.07
−6 dB height (elevational) (mm)	3.92 ± 0.05	4.11 ± 0.05	0.95 ± 0.02
−6 dB Beam Area (mm^2)	3.31 ± 0.15	3.15 ± 0.15	1.05 ± 0.07
Power (mW)	55.9 ± 4.5	26.4 ± 2.3	2.12 ± 0.25
I_{sata} (W/cm^2)	1.69 ± 0.15	0.84 ± 0.08	2.01 ± 0.23

The scanner was an Acuson Sequoia with 6L3 scanhead operating in M-Mode at 5.0 MHz and 5.0 cm focal depth.

Table 4. Test of long-term stability of values of primary acoustic output parameters measured in TM Liquid. An initial set of measurements were made followed 6 mo later by a second set

Parameter	Initial value in TM liquid	Value in TM Liquid 6 mo later
PII_{max} ($\mu J\ cm^{-2}$)	34.9 ± 3.6	38.2 ± 3.6
f_c (MHz)	4.91 ± 0.03	4.94 ± 0.03
PD (μs)	0.29 ± 0.02	0.30 ± 0.02
I_{SPTA} ($mW\ cm^{-2}$)	21.3 ± 1.1	23.3 ± 1.1
I_{SPPA} ($W\ cm^{-2}$)	121 ± 8	127 ± 8
p_r (MPa)	1.91 ± 0.07	1.78 ± 0.07
p_c (MPa)	2.56 ± 0.07	2.61 ± 0.07
MI equivalent	0.86 ± 0.03	0.80 ± 0.04

An Acuson Sequoia was employed with a 6L3 scanhead operating in M-mode at 5.0 MHz and 5.0 cm focal depth.

"transmit power." To avoid any confusion associated with the use of the word power and in keeping with the definitions included in the AOMS, this control will be referred to as "drive voltage amplitude." The drive voltage amplitude directly controls the amplitude of the pressure signal at its point of creation. Because nonlinear propagation effects are strongly dependent on amplitude, decreasing the drive voltage amplitude from full output should have a substantial effect upon the differences between parameters measured in TM liquid and those measured in water with derating applied. In fact, it has been suggested that the errors associated with derating could be eliminated by extrapolating results from low drive voltage amplitudes to high drive voltage amplitudes (Christopher 1999; Bigelow and O'Brien 2002; Duncan et al. 2003).

Manufacturers typically display the value of the drive voltage amplitude in reference to the maximum drive voltage amplitude (either as a percentage of the maximum or decibels below the maximum). Therefore, the results of this section are presented in terms of the fraction of maximum drive voltage amplitude for a particular scanner and configuration. In the case of the Acuson Sequoia, the drive voltage amplitude control is labeled in decibels with full output of 0 dB decreasing to −30 dB relative to the maximum output. The hydrophone was kept in the position of global maximum PII for the configuration with full output. Then the drive voltage amplitude control was adjusted and waveforms recorded for every possible setting of this control.

The waveforms recorded at the various drive voltage amplitudes were analyzed to determine the PII, p_c, and p_r of each waveform. Under linear propagation of ultrasound, one would expect the measured pressure at any particular point in the acoustic field to vary in direct proportion to the drive voltage amplitude. Graphs of p_r versus drive voltage amplitude are shown in Fig. 12. Since the PII and other measures of the intensity of ultrasound vary as pressure squared, one would expect that a graph of the PII versus fraction full voltage amplitude to display a quadratic nature. To better allow for direct examination of the results in comparison to this expectation, the abscissa of the graph of PII (Fig. 13) at various drive voltage is the square of the fraction full voltage amplitude.

DISCUSSION AND SUMMARY

The maximum PII for this configuration was measured to be almost a factor of two greater in TM liquid than in water with derating applied. Because of their direct dependence on the PII, the I_{SPTA} and I_{SPPA} were similarly underestimated in water with derating applied. As could be expected, the center frequency and pulse duration are quite similar in TM liquid and in water with derating applied. Both of these parameters are slightly smaller in TM liquid than in water with derating. For the center frequency, this is explained by the presence of attenuation in the TM liquid. As a pulse propagates in a lossy medium, it undergoes "beam-hardening" as the higher frequency content of the pulse is attenuated by a greater amount than the lower frequency content. Thus, the frequency of the upper −3 dB spectral point shifts to lower frequency as the ultrasound signal propagates. The slight decrease in pulse duration (PD) as measured in TM liquid can be understood from the fact that the beginning and end of the pulse in TM liquid are similar in amplitude to the corresponding amplitudes in water with derating applied. Since the PD is defined in terms of the times at which the integral of the intensity is 10% and 90% of the PII, these times change somewhat in TM liquid. The mechanical index (the rarefactional pressure at the location of maximum PII divided by the square

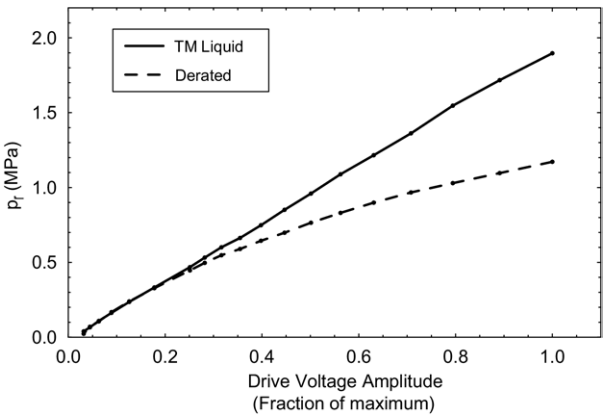

Fig. 12. Variation of p_r with drive voltage amplitude, measured at the location of the global maximum PII at full drive voltage amplitude.

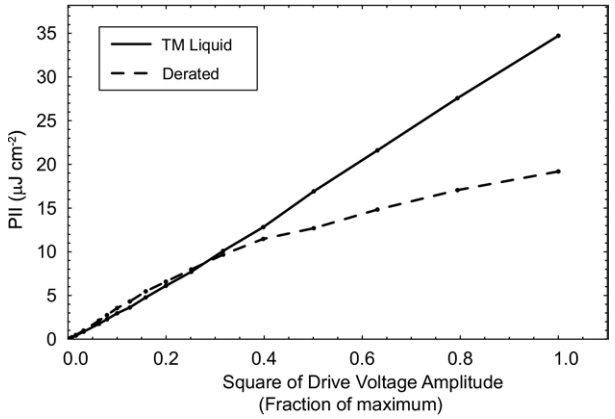

Fig. 13. Variation of PII with drive voltage amplitude, measured at the location of the global maximum PII at full drive voltage amplitude.

root of the center frequency) is also severely underestimated in water, with a value of 0.9 in TM liquid and only 0.5 in water.

The ratio of the PII in TM liquid to the derated PII in water increases linearly with distance from the source. The same is true of the ratio of the rarefactional pressure. However, the derated p_c axial profile measured in water is close to that measured in TM liquid. Figure 10 displays the ratio of the PII measured in TM liquid to that measured in water with derating applied (solid curve). As can be seen in Fig. 10, the ratio between maximum compressional pressure in TM liquid and the derated value in water remains close to equality at all depths. It is interesting to note that the derating method appears (at least in this configuration) to fairly accurately represent the compressional pressure. A solid theoretical understanding of the pressure asymmetry needs to be developed before further conclusions can be reached on this subject.

The AOMS requires measurement values of all parameters to be those that occur at the location of the maximum derated PII. Note that neither the rarefactional pressure nor the compressional pressure necessarily reaches its maximum at the location of maximum PII. Values of the absolute (global) maximum compressional and rarefactional pressures along with a repetition of the values of the peak rarefactional and compressional pressure are provided in Table 2 A numerical study by Christopher (1999) suggests that the use of the global maximum peak rarefactional pressure in the definition of the MI may lead to values that better estimate the value in tissue. In the case of this configuration, however, the global maximum rarefactional pressure is still significantly underestimated in water with derating applied when compared with measurements in TM liquid. The ratio between the value in water with derating to that in TM liquid is only slightly less for the global maximum rarefactional pressure (1.48 ± 0.05) than it is for the peak rarefactional pressure at the location of maximum PII (1.62 ± 0.07).

As can be observed from Fig. 11 and Table 3, the geometrical values related to the physical "size" of the beam (perpendicular to the beam axis) are nearly identical in TM liquid and in water with derating applied. These parameters are important in determining resolution and other imaging parameters.

The results of our study show a marked difference between values obtained in TM liquid and those in water with derating applied. As shown in Fig. 13, the PII in TM liquid does approximately vary as the square of the drive voltage amplitude. This is not the case for the PII measured in water with derating applied. At low drive voltage amplitudes, the derated water values actually are quite close to those measured in TM liquid. However, at about 50% of full drive voltage amplitude (corresponding to 0.25 on the abscissa of Fig 13), the value of the derated PII measured in water begins to be less than the value in TM liquid. This difference between values in TM Liquid and the corresponding derated value obtained in water increases as the drive voltage amplitude is increased beyond 50% of its maximum, reaching the previously discussed factor of 1.86 discussed above and presented in Table 1

The p_r (shown in Fig. 12) varies nearly proportionally to the fraction of full drive voltage amplitude in TM liquid. Again, in water, the p_r is linear at low drive voltage amplitudes but begins to deviate from proportionality, becoming less than proportional to the drive voltage amplitude at high drive voltage amplitudes at about 30% of the maximum drive voltage amplitude. The maximum compressional pressure (p_c) (shown in Fig. 14) is not proportional to drive voltage amplitude in TM liquid nor in water; in both media, the peak compres-

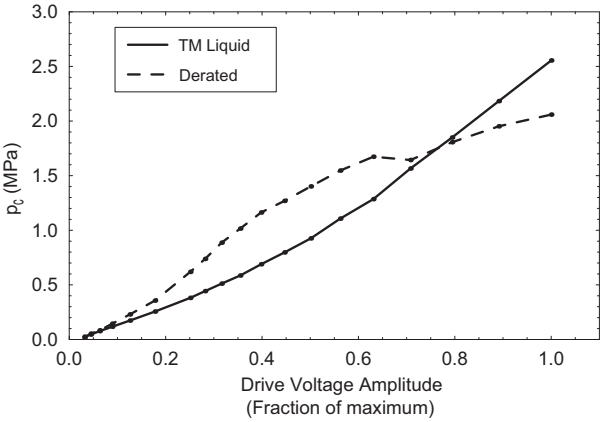

Fig. 14. Variation of p_c with drive voltage amplitude, measured at location of the global maximum PII at full drive voltage amplitude.

sional pressure increases faster with drive voltage amplitude than a simple proportionality. In water, there is a point at about 60% of maximum applied power at which the compressional pressure plateaus. This is probably due to saturation of the actual (underated) pressure in water. The figures in this section clearly present the nonlinear nature of ultrasound propagation, especially in water. For a large range of drive voltage amplitudes, the pressure and intensity (as measured by the PII) do not change in the same proportion as the first or second power of the drive voltage amplitude. This is a situation in which you can double the input to a system without necessarily doubling the output of that system, the essence of a nonlinear system.

One may question whether the value displayed by the scanner accurately portrays the amplitude of the voltage signal used to excite the transducer elements. As a test of this accuracy, the signal from the pick-up coil usually used as a trigger to the oscilloscope was also measured over the range of drive voltage amplitudes. The pick-up coil is sensitive to the actual voltage signal used to excite the transducer elements. The peak-to-peak amplitude of the signal from the pick-up coil varied exactly as predicted by the setting of this control on the scanner, suggesting that the values provided by the scanner are an accurate depiction of the voltage used to excite the transducers.

The apparatus described in this work allows for direct measurement of acoustic output parameters in a stable tissue mimicking liquid. This eliminates the need to perform derating which has a high likelihood of introducing significant errors by not including the nonlinear loss and saturation effects that can occur in water. Comparison of values of acoustic output parameters in TM liquid with derated values obtained in water for a single configuration indicate that the derated values may substantially underestimate the TM liquid values. A forthcoming manuscript will expand on these measurements with results from a wide variety of configurations.

Acknowledgments—This Study was supported in part by NIH grants R41GM54377, T32CA09206 and K25EB004358.

REFERENCES

AIUM/NEMA. Acoustic Output Measurement Standard for Diagnostic Ultrasound Equipment. American Institute of Ultrasound in Medicine, Laurel, MD, and National Electrical Manufacturers Association, Rosslyn, VA, 2004.

Berntsen J. Numerical calculations of finite amplitude sound beams. In Hamilton MF, Blackstock DT, ed. Frontiers of Nonlinear Acoustics. Proceedings of the 12th ISNA, Elsevier Applied Science, 1990. pages 191–196.

Bigelow TA, O'Brien Jr. WD. Experimental evaluation of indicators of nonlinearity for use in ultrasound transducer characterizations. Ultrasound Med Biol 2002; 28:1509–1520.

Brekhovskikh LM. Waves in Layered Media. Academic Press, New York, NY, second edition, 1980. Translated by Robert T. Beyer.

Cahill MD, Humphrey VF. A theoretical investigation of the effect of nonlinear propagation on measurements of mechanical index. Ultrasound Med Biol 2000;26:433–440.

Christopher T. Computing the mechanical index. J Ultrasound Med 1999;18:63–68.

Divall SA, Humphrey VF. Finite difference modelling of the temperature rise in non-linear medical ultrasound fields. Ultrasonics 2000; 38:273–277.

Duck FA. Nonlinear acoustics in diagnostic ultrasound. Ultrasound Med Biol 2002;28:1–18.

Duncan T, Humphrey VF, Duck, FA. A numerical comparison of nonlinear indicators for diagnostic ultrasound fields. In: Proceedings of the World Congress on Ultrasonics 2003, World Congress on Ultrasonics, 2003:85–88.

MacDonald MC, Madsen EL. Acoustic measurements in a tissue mimicking liquid. J Ultrasound Med 1999;18:55–62.

Marple Jr SL. Digital spectral analysis: With applications. Prentice Hall, Inc., Englewood Cliffs, NJ, 1987.

Selfridge AR. Approximate material properties in isotropic materials. IEEE Trans Sonics Ultrason 1985;SU-32:381–394.

Stiles TA, Madsen EL, Frank GR, Deihl TF, Lucey JA. Tissue-mimicking liquid for use in exposimetry. J Ultrasound Med 2005: 24:501–516.

Szabo TL, Clougherty F, Grossman C. Effects of nonlinearity on the estimation of in situ values of acoustic output parameters. J Ultrasound Med 1999;18:33–41.